

1 **A structural property for reduction of biochemical networks**

2 Anika Küken ¹, Philipp Wendering ¹, Damoun Langary ², Zoran Nikoloski ^{1,2*}

3 ¹ Bioinformatics, Institute of Biochemistry and Biology, University of Potsdam, Potsdam,
4 Germany

5 ² Systems Biology and Mathematical Modeling, Max Planck Institute of Molecular Plant
6 Physiology, Potsdam, Germany

7 *Correspondence to: nikoloski@mpimp-golm.mpg.de.

8

9 **Abstract**

10 Large-scale biochemical models are of increasing sizes due to the consideration of interacting
11 organisms and tissues. Model reduction approaches that preserve the flux phenotypes can
12 simplify the analysis and predictions of steady-state metabolic phenotypes. However, existing
13 approaches either restrict functionality of reduced models or do not lead to significant decreases
14 in the number of modelled metabolites. Here, we introduce an approach for model reduction
15 based on the structural property of balancing of complexes that preserves the steady-state fluxes
16 supported by the network and can be efficiently determined at genome scale. Using two large-
17 scale mass-action kinetic models of *Escherichia coli*, we show that our approach results in a
18 substantial reduction of 99% of metabolites. Applications to genome-scale metabolic models
19 across kingdoms of life result in up to 55% and 85% reduction in the number of metabolites
20 when arbitrary and mass-action kinetics is assumed, respectively. We also show that
21 predictions of the specific growth rate from the reduced models match those based on the
22 original models. Since steady-state flux phenotypes from the original model are preserved in

23 the reduced, the approach paves the way for analysing other metabolic phenotypes in large-
24 scale biochemical networks.

25 **Keywords**

26 Metabolic networks, network reduction, constraint-based modeling

27

28 **Introduction**

29 Advances in phenotyping, quantitative genetics methods, and systems biology have helped
30 characterize function of genes embedded in different types of biochemical networks ¹⁻³.

31 Generation of large-scale stoichiometric models, capturing the metabolism of individual cell
32 types and their interactions in an organism or communities ¹, has propelled the development of
33 computational approaches for prediction and analysis of metabolic phenotypes ⁴. The sheer size
34 of genome-scale metabolic networks indisputably leads to computational and numerical
35 challenges when employing them to predict and analyse metabolic phenotypes, particularly
36 when these networks are endowed with enzyme kinetics ⁵⁻⁷. Against this background we ask:
37 Can large-scale biochemical models be reduced in an unbiased, i.e. fully automated fashion,
38 while still guaranteeing that the steady-state flux phenotypes are preserved in the resulting
39 models of smaller size?

40 There already exist several frameworks and theories to reduce biochemical models ^{8,9}. These
41 approaches can be categorized based on different criteria: (i) whether they only employ the
42 structure of the network (i.e. stoichiometry of biochemical reactions) ⁹⁻¹³ or also consider the
43 kinetics of reaction fluxes ¹⁴⁻²³, (ii) whether they approximate or provide one-to-one
44 correspondence of the steady-state properties between the original and reduced network ^{10,23-}
45 ²⁵, and (iii) whether the reduction process is fully automated, i.e. unbiased, or semi-automated
46 (i.e. requires user input) ⁹.

47 Reduction approaches rooted in the constraint-based modelling framework have been
48 successfully employed to arrive at reduced models that approximate *steady-state flux*
49 *properties* of large-scale metabolic networks. One group comprises approaches based on user-
50 specified input, consisting of pre-selected metabolites, reactions, and functions (e.g. biomass
51 production) that must be present or supported by the reduced model and, thus, result in reduced
52 models biased by the user's input ^{24–26}. Other approaches in this group start with user-defined
53 subsystems that are subsequently connected (and further refined) to obtain a minimal model
54 that can fulfil a pre-specified function ²⁷. In contrast, using ideas from reaction coupling ²⁸, a
55 recent unbiased approach provides an efficient reduction of stoichiometric models by reaction
56 removal, while ensuring one-to-one correspondence between the elementary flux modes of the
57 original and reduced model ¹⁰. Since these approaches do not consider kinetics of reaction flux,
58 they remain silent about the effects that the reduction has on the concentrations of the remaining
59 metabolites.

60 Approaches for reduction of models with mass action kinetics are particularly important to
61 solve or approximate different reaction mechanisms (e.g. Michaelis-Menten, Hill) ^{16,29}. They
62 usually invoke the quasi-steady state assumption (QSSA), whereby the modelled components
63 can be grouped into those with small concentrations, referred to as intermediates, and those
64 with large concentrations (i.e. substrates and products), such that the network displays two (or
65 more) timescales. Invoking QSSA implies that the intermediates, that change on the fast time
66 scale, are expressed as functions of the slow components ¹⁶. Therefore, these intermediates are
67 eliminated from the original network and, then, the reduced network, capturing the slow
68 dynamics, is further analysed. Application of QSSA is not straightforward since it requires data
69 on kinetic parameters that are challenging to obtain at a genome-scale level ³⁰. Therefore, such
70 approaches cannot be analytically carried out ²⁹, and often involve approximations that lead to
71 inaccuracies of estimations.

72 One unbiased technique to eliminate a component in mass action networks requires that the
73 component appears only as a sole substrate or product in the reactions in which it participates
74 ²³. Assuming steady state, the concentration of such a component can be readily expressed as
75 a function of the concentrations of the remaining components. This approach guarantees
76 correspondence between the conservation laws of the original and reduced network and the
77 respective numbers of positive steady states ²³. This idea has been generalized to allow linear
78 removal of some subsets of components that appear only with stoichiometry at most one in any
79 reaction of a given network endowed with mass action kinetics ¹⁴. Yet, structural conditions
80 ensuring that the steady-state flux spaces of the reduced network are subset of the reduced
81 network by removal of components of any stoichiometry in networks endowed with arbitrary
82 kinetics remain elusive.

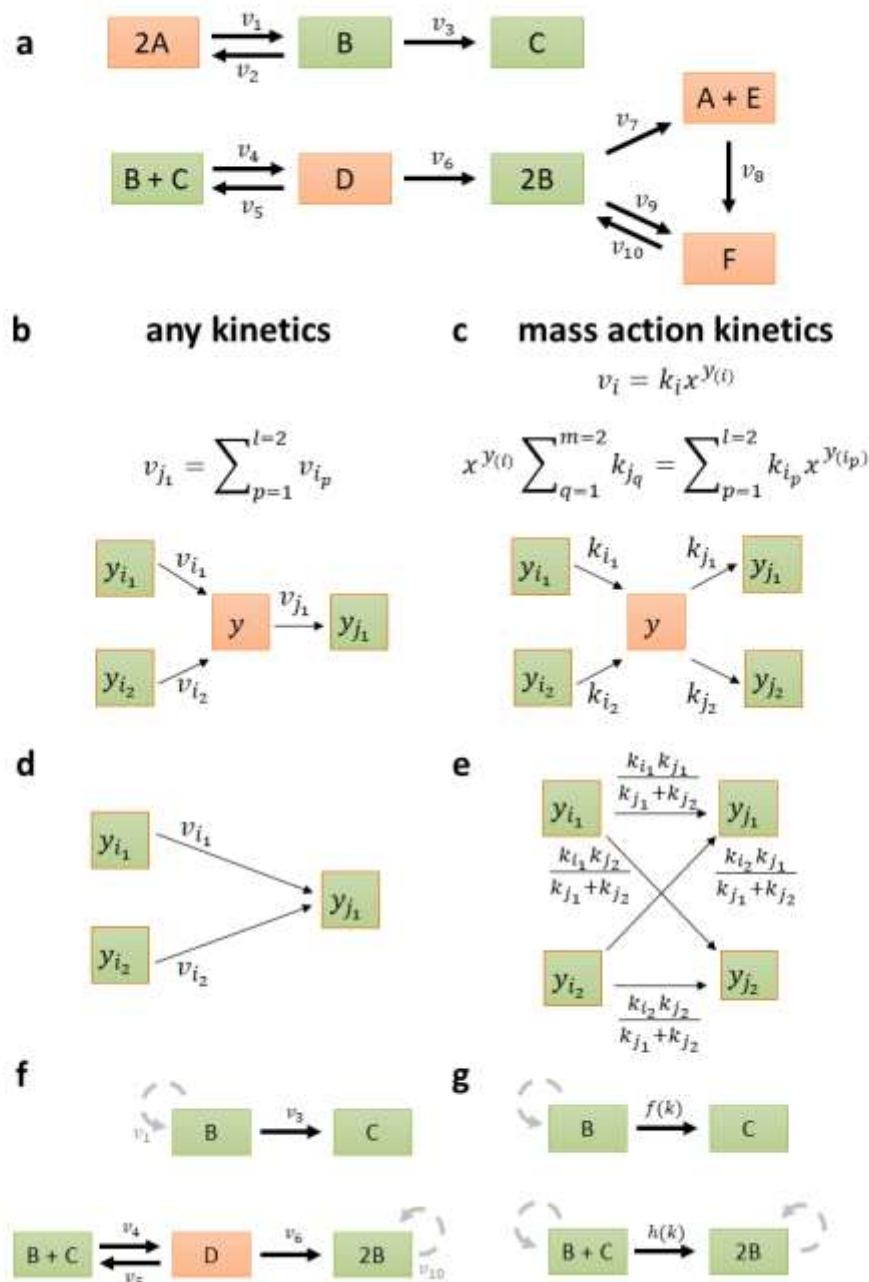
83 Here we identify such a structural property for model reduction and show that it can be
84 efficiently computed and applied in genome-scale metabolic networks from organisms across
85 the kingdoms of life. The condition allows consideration of biochemical constraints and can,
86 therefore, be invoked with or without assumptions on optimized biological function. The key
87 advantage of the structural condition is that it can be applied to large-scale biochemical
88 networks endowed with mass action kinetics, and under some restrictions, to networks
89 endowed with arbitrary kinetics, while guaranteeing that the steady-state flux phenotypes of
90 the original model are preserved in the reduced.

91 **Results and Discussion**

92 **Balancing of complexes as a structural condition for network reduction**

93 To illustrate the condition, we first introduce some key concepts from stoichiometric modelling
94 of biochemical networks. A biochemical network is composed of irreversible reactions through
95 which biochemical species acting as substrates are transformed into products. The biochemical

96 network on Fig. 1a is composed of ten reactions that transform six species. The network
97 structure is described by nodes that denote complexes, corresponding to the left- and right-
98 hand sides of the considered reactions, and edges representing the reactions. Therefore, the
99 network on Fig. 1a contains eight complexes connected by ten reactions. The incoming and
100 outgoing neighbourhoods of a complex are given by the complexes to which it is directly
101 connected via incoming and outgoing reactions, respectively. For instance, the incoming
102 neighbourhood of complex 2B is composed of complexes D and F, and the outgoing
103 neighbourhood comprises A+E and F. The stoichiometric matrix of the network, N , is then
104 given by the product of the matrix, Y , describing the species composition of complexes and the
105 incidence matrix, A , of the corresponding directed graph (Methods, Supplementary Fig. S1)
106 ^{31,32}. In addition, the reactions are weighted by non-negative numbers which correspond to
107 fluxes of a steady-state flux distribution, v , which satisfies $Nv = 0$. The steady-state condition
108 implies that the concentrations of species are invariant in time, i.e. the species are *balanced*,
109 whereby the production and consumption rates are the same.



110

111 **Figure 1. Balanced complexes for network reduction.** (a) Toy example network borrowed
 112 from Shinar and Feinberg³³, including six species, A – F, eight complexes, depicted as
 113 rectangles, and ten reactions, with rates v_1 - v_{10} , each connecting two complexes. Balanced
 114 complexes are shown in orange, while non-balanced complexes are depicted in green. Balanced
 115 complexes 2A, A+E, and F have one outgoing reaction, while the balanced complex D has
 116 more than one outgoing reaction. Structural motif allowing removal of the balanced complex

117 y **(b)** with single outgoing reaction, for an arbitrary kinetics and **(c)** with multiple outgoing
118 reactions, for mass action kinetics. Removal of the complex amounts to substitution of
119 variables, either with respect to reaction rates v or monomials of species concentrations x^y ,
120 which can be represented by **(d)** network rewriting, for arbitrary kinetics and **(e)** additional
121 scaling of reaction rate constants, with mass action kinetics. **(f)** Reduced network obtained by
122 removing the balanced complexes $2A$, $A+E$, and F ; the loop reactions are shown in grey since
123 they do not contribute to the stoichiometric matrix. **(g)** Reduced network obtained from the
124 network in panel **(f)** after removal of the balanced complex D , assuming mass action. For
125 simplicity, the rate constants are given as functions $f(k)$ and $h(k)$.

126

127 An analogous condition on balancing can be defined for a single complex: Given a biochemical
128 network, a complex is balanced in a set of steady-state flux distributions S if the sum of fluxes
129 of its incoming and outgoing reactions is the same for every flux distribution in S . Clearly,
130 complexes that act as sinks or sources, that only have incoming or outgoing reactions,
131 respectively, cannot be balanced in a network without blocked reactions (i.e. reactions which
132 carry no flux in every steady state the network supports). Further, a complex is considered
133 *trivially balanced* if it includes a species that appears in no other complex in the network. This
134 result is a consequence of the balancing of species due to the steady state assumption. A
135 balanced complex that includes species all of which appear in other complexes are termed *non-*
136 *trivially balanced*. For instance, complex C cannot be balanced as it is a sink, while D , $A+E$,
137 and F are trivially balanced since species D , E , and F appear only in these complexes that have
138 both incoming and outgoing reactions. Note that our definition of trivially balanced complexes
139 extends the notion of an intermediate species in other reduction approaches²³. Finally, $2A$ is a
140 non-trivially balanced complex, since A appears in two complexes of which one, $A+E$, is

141 trivially balanced. In fact, by considering only the steady-state conditions, it is the interlinking
142 of species into complexes that contributes to the formation of balanced complexes.

143 For a set S of steady-state flux distributions, every balanced complex can be readily identified
144 by constraint-based modelling (Methods). The approach amounts to determining that the
145 minimum and maximum total fluxes around a complex are zero for all steady-state flux
146 distributions in the set S . These conditions can be verified by linear programming that is
147 efficient even for large-scale networks (Methods). The identification of balanced complexes
148 can be further streamlined by easy screening of trivially balanced as well as sink and source
149 complexes.

150 Networks in which all complexes are balanced are termed complex balanced, and they can be
151 identified by calculating the structural property of deficiency³⁴. Seminal theoretical results
152 pinpoint that complex balanced networks do not exhibit exotic properties, like multistationarity
153 and oscillations. However, it has not yet been addressed how one can identify individual
154 balanced complexes and what the implications of their presence in the network are with respect
155 to the capacity to exhibit particular phenotypic properties.

156 We next ask if balanced complexes are relevant for reduction of networks which are not
157 complex balanced. To answer this question, we first consider the scenario with a network
158 endowed with arbitrary kinetics. If a balanced complex has only one outgoing reaction, then
159 the flux of this reaction can be expressed as a sum of the fluxes of incoming reactions. The
160 balanced complex can then be safely removed since the flux of the outgoing reaction can be
161 substituted with the respective sum of fluxes of the incoming reactions for the balanced
162 complex. This is concomitant to introducing a bipartite directed clique, connecting each
163 complex in the incoming neighbourhood with the complex in the outgoing neighbourhood (Fig.
164 1b,d). . Note that any loop edges introduced by this transformation can be removed, since they

165 do not contribute to the balancing equations. For instance, A+E, F, and 2A can be removed as
166 balanced complexes, resulting in the network on Fig. 1f; however, this cannot be done for the
167 balanced complex D since it has more than one outgoing reaction. Since the removal of
168 complexes in this way results in expressing one flux as a sum of others, the reduced network
169 is unique and does not depend on the order of removing the balanced complexes. A similar
170 idea has been used in the unbiased efficient reduction of stoichiometric models ¹⁰, however,
171 based on the coupling of reactions around balanced species and without the rewiring of
172 reactions.

173 Attempting to remove a balanced complex with more than one outgoing reaction fails in
174 general; however, under the constraint that all outgoing reactions are fully coupled (i.e. their
175 flux ratio in every steady state is a unique constant) all outgoing reaction fluxes collapse into
176 one and the balanced complex can be removed. Interestingly, this condition is trivially met for
177 networks endowed with mass action kinetics, since the ratio of fluxes of reactions outgoing
178 from any complex is given by the ratio of the respective rate constants. Importantly, this
179 removal can be carried out even if values for the rate constants are not specified, since the ratio
180 is ensured to be constant. Therefore, under mass action, a balanced complex can be removed
181 by introducing a bipartite directed clique of reactions with rescaled kinetic constants (see
182 Methods, Fig. 1c,e). For instance, the balanced complex D can be removed, like the other
183 balanced complexes in the network, resulting in a mass action network with fewer complexes
184 and species, and reactions with modified kinetic parameters, as shown in Fig. 1g.

185 The usage of balanced complexes to reduce networks with mass action kinetics generalizes the
186 removal of trivially balanced complexes in which species appear in a single complex with
187 stoichiometry of one ²³. However, the proposed approach allows removal of species that
188 participate in any number of complexes with any stoichiometry, provided they appear only in
189 balanced complexes. It also provides a sound extension of a reduction approach in which

190 complexes are--arbitrarily--assumed to be balanced ¹⁸ – and leads to biases in the model
191 reduction since the complexes are not demonstrated to be balanced. In our approach, the
192 conservation laws in the original network hold in the reduced, but not necessarily vice versa
193 (see Methods). Therefore, if the original network has at most one positive steady state for any
194 rate constants and values for the conservation moieties, then the reduced model also has at most
195 one positive steady state for the rescaled rate constants ²³. Hence, analysis of the reduced model
196 can help identify if multistationarity for the concentration of remaining species is precluded in
197 the original, larger model if seminal, well-established conditions apply ³⁴. Note that, the
198 removal of balanced complexes may result in removal of species, but may lead to an increase
199 in the number of reactions. Most importantly, the steady-state concentration of any removed
200 species in the process of model reduction can be expressed as a function of the concentrations
201 of the species in the reduced model (Supplementary Fig. S2).

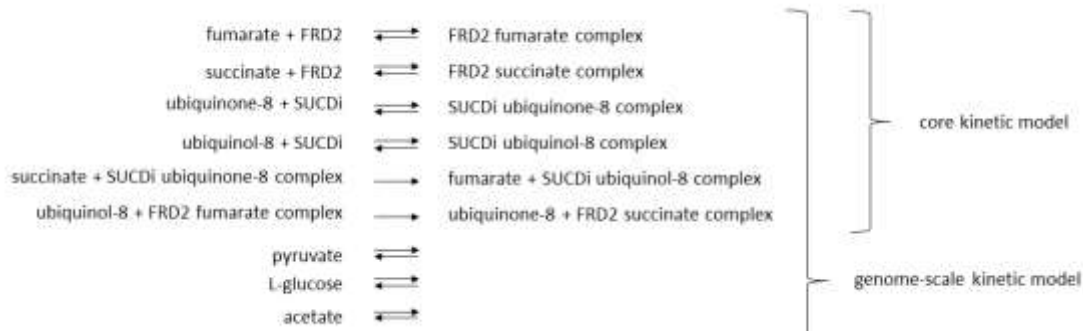
202 **Reduction of a large-scale kinetic model of *Escherichia coli* metabolism**

203 To verify that the proposed approach could lead to reduction of metabolic networks endowed
204 with mass action kinetics, we used the genome-scale ⁷ and the so-called core ³⁵ kinetic
205 metabolic models of *E. coli*. The core model is composed of 828 species, 1474 irreversible
206 reactions, and 1190 complexes, while the genome-scale model consist of 3002 species, 5237
207 irreversible reactions, and 4371 complexes. Relying solely on the structure of the network, we
208 identified 484 and 1639 balanced complexes in the core and genome-scale kinetic models,
209 respectively, of which 77.7% and 75.4% were trivially balanced. For instance, the complexes
210 'Phosphoenolpyruvate + FBP- Phosphoenolpyruvate -complex', 'ACALD-acetaldehyde-
211 NAD-CoA-complex', and '3-phospho-glycerate + PGK-3-phospho-glycerate-complex' are
212 trivially balanced since the respective enzyme-substrate biochemical complexes appear only in
213 these network complexes. In addition, the complex '3-phospho-glycerate + ICL' is non-
214 trivially balanced, since the species 3-phospho-glycerate appears only in two complexes ('3-

215 phospho-glycerate + ICL' and '3-phospho-glycerate + PGK-3-phospho-glycerate-complex' x)
216 and the complex '3-phospho-glycerate + PGK-3-phospho-glycerate-complex' is trivially
217 balanced. From the 484 and 1639 balanced complexes 23% and 26% had only one outgoing
218 reaction; for instance, 'L-aspartate + PRASCS-ATP-complex', 'ATP + PRASCS', and
219 'glucose-6-phosphate + FBP' are balanced complexes with such properties (see Supplementary
220 Figure S3). The removal of such balanced complexes led to a decrease in the number of species
221 by ~14% in comparison to both investigated kinetic models. Both models consider elementary
222 reaction steps and, therefore, model species can be of three types: metabolite, enzyme or
223 metabolite-enzyme biochemical complex. We observed that ~95% of the species removed
224 denoted species that represent metabolite-enzyme biochemical complexes. This is in line with
225 the commonly applied assumption in deriving kinetics that are based on mass action (e.g.
226 Michaelis-Menten), and is due to the fact that metabolite-enzyme complexes, as species,
227 participate in single network complexes that are consequently trivially balanced (as illustrated
228 in the examples above). When considering the additional restriction due to mass action kinetics,
229 we could apply the approach in a second round of reduction. This led to the identification of
230 694 and 2708 additional non-trivial balanced complexes in the core and genome-scale kinetic
231 model, respectively. Removal of these balanced complexes led to ~99% decrease in the number
232 of species in comparison to the original model for the core as well as the genome-scale model.
233 Therefore, the approach does lead to a substantial reduction in the number of species even when
234 only the structure of the network was employed.

235 The reduced core kinetic model comprises: fumarate, succinate as well as ubiquinone-8 and
236 ubiquinol-8, interconverted by fumarate reductase (FRD2) and succinate dehydrogenase
237 (SUCDi) together with the related substrate-enzyme complexes (Fig.2). In the reduced
238 genome-scale model extracellular pyruvate, acetate, and L-glucose as well as enzymes
239 exchanging those metabolites with the environment extend the set of species around fumarate

240 reductase and succinate dehydrogenase that are found in the reduced core kinetic model (Fig.
241 2). Therefore, the steady-state concentrations of all other metabolites in these kinetic models
242 can be expressed as functions of the few species that are present in the reduced model.



244 **Figure 2. Illustration of the reduced core and genome-scale kinetic models obtained by**
245 **reduction of a mass action kinetic model.** The reduced core kinetic model comprises ten
246 components and ten reactions, while the reduced genome scale kinetic model consists of 13
247 compounds and 16 reactions. (fumarate reductase - FRD2, succinate dehydrogenase - SUCDi).
248 The concentration of the components present in the reduced networks can be used to model the
249 concentration of all other components in the original networks.

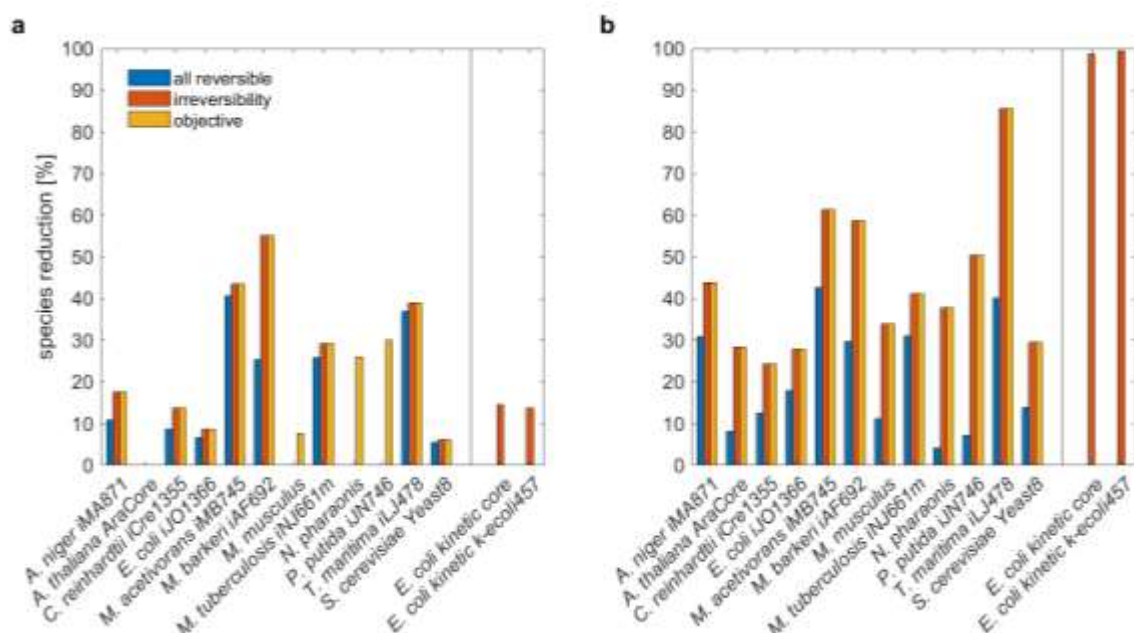
250

251 **Reduction of large-scale stoichiometric metabolic networks**

252 Motivated by the findings from the reduction of the core and genome-scale kinetic models of
253 *E. coli* metabolism, we next employed the proposed approach to inspect the reduction in the
254 number of species in genome-scale metabolic models of different organisms. To this end, we
255 used the metabolic networks of twelve organisms to compare and contrast the reductions for
256 the following scenarios: (i) all reactions are assumed to be reversible in contrast to the case
257 when irreversibility constraints, included in the original models, are used, (ii) all reactions
258 follow arbitrary kinetics or their fluxes are described by mass action kinetics, (iii) balanced

259 complexes are determined with respect to the set of steady-state flux distributions compatible
 260 with reversibility in comparison to steady-state flux distributions at optimal specific growth
 261 rate. Note that reversible reactions are split into two irreversible reactions before applying the
 262 approach.

263 With arbitrary kinetics of reaction fluxes, the general observation was that invoking
 264 irreversibility led to only a small increase (< 7%) in the number of removed species across all
 265 organisms (Fig. 3a, Supplementary Table S1). The model of *M. barkeri* is an exception to this
 266 finding, with 30% increase in species reduction when considering reaction irreversibility. In
 267 addition, imposing constraints on biomass had negligible additional effect on the balanced
 268 complexes in majority of the networks, except in the models of *P. putida* and *N. pharaonis*, for
 269 which there was an increase by 26 and 30% in the number of removed species, respectively
 270 (Fig. 3a). This finding demonstrated that the balanced complexes are a property of the network
 271 structure and steady-state constraint, rather than due to optimality conditions imposed.



272
 273 **Figure 3. Reduction of genome-scale metabolic networks.** Genome-scale metabolic models
 274 of twelve organisms from all kingdoms of life are used in the reduction (a) with arbitrary

275 kinetics and **(b)** assuming mass action kinetics. The analysis also includes two large, mass-
276 action kinetic models of *E. coli*. Shown is the percentage of reduction in the number of species
277 with respect to the original model.

278

279 Consideration of mass action kinetics led to an increase in model reduction of, on average, 26%
280 in comparison to the case of arbitrary kinetics when all reactions are considered reversible (Fig.
281 3a, b). In contrast to the case of arbitrary kinetics, the assumptions of reaction irreversibility
282 has a large effect on the reduction in the number of species in comparison to the case when all
283 reactions are assumed to be reversible (Fig. 3b). On average, we observed 23% increase in
284 species reduction when reaction irreversibility is considered. Finally, imposing constraints on
285 biomass had no effect on the balanced complexes and, thus, on the number of removed species,
286 when mass action was considered (Fig. 3b).

287 Altogether, when irreversibility for reactions in the original model was considered, the
288 proposed approach led to no reduction in the number of species in the *Arabidopsis thaliana*
289 core, *M. musculus*, *N. paharaonis* and *P. putida* model and reached up to 55.1% reduction in
290 the model of *M. barkeri*. On average we observed 18% of species being removed across all
291 considered networks. Instead, when mass action kinetics was considered, we found a reduction
292 between 24.3% for *E. coli* to 85.7% in *T. maritima*, with an average of 44% across the
293 considered models. These results demonstrated that substantial reduction in the number of
294 removed species is possible, while ensuring that the key network properties at steady state are
295 matched between the original and reduced network. In addition, the reduction eliminated up to
296 17 (12%) species which enter complexes with stoichiometry larger than one (Supplementary
297 Table S2), which is not possible with the existing approaches.

298 As a general note, the differences in the reduction of the considered models is due to the
299 differences in the number and positioning of balanced complexes with the specific motif of
300 having one outgoing – many incoming reactions (or *vice versa*) in the specific scenarios
301 considered. In comparison to the reduction of the large-scale mass action model of *E. coli*, its
302 counterpart with arbitrary kinetics can be reduced to a smaller degree since its balanced
303 complexes that have the motif structure for reduction are subset of such balanced complexes
304 when mass action is employed. Furthermore, the differences between the scenarios are due to
305 the additional constraints imposed in each of the scenarios.

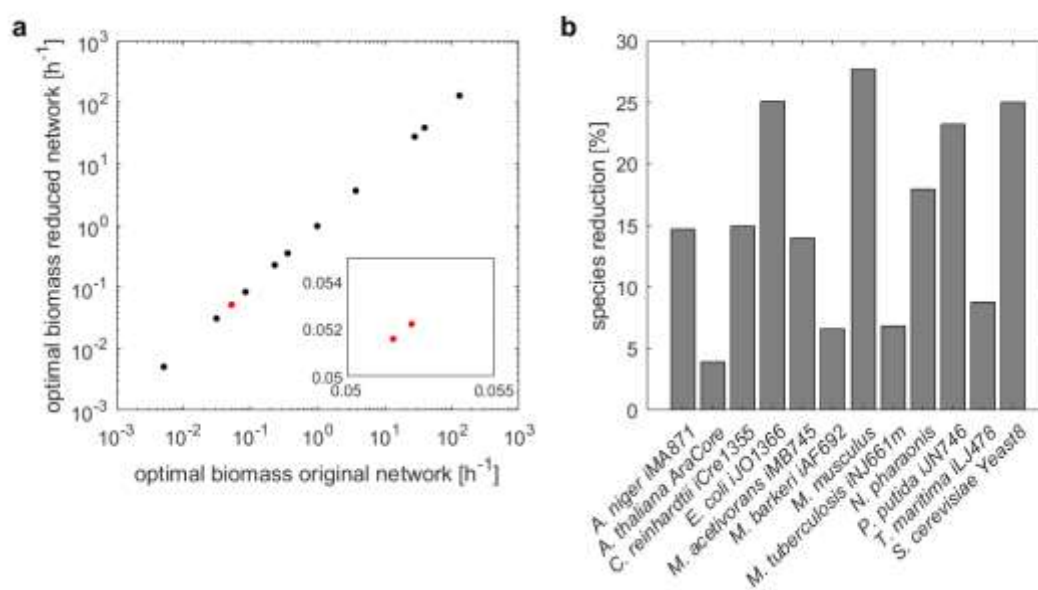
306 Next, we investigate compartment-wise species reduction between the original and reduced
307 models, considering reaction irreversibility and mass action kinetics. In doing this analysis, we
308 determined the balanced complexes in the entire network, and then investigated the effect of
309 the reduction by using information about compartments in the respective models. The general
310 observation was that models comprising extracellular space show large reduction for this
311 compartment. The reduction ranged from 26% for *N. pharaonis* to 100% in *T. maritima*
312 (Supplementary Table S3). On average, the reduction over the ten models including
313 extracellular space as a compartment was 65.5%. The average reduction for the cytoplasmic
314 part of bacterial and archaea models was 49%. Compartmented models of *S. cerevisiae*, *C.*
315 *reinhardtii* and *A. thaliana* showed largest reduction in mitochondria, chloroplast and cytosol,
316 respectively (Supplementary Table S3).

317 Using the two genome-scale metabolic models of *E. coli* and *S. cerevisiae* we compared the set
318 of metabolites in the original and reduced models using Jaccard similarity (see Methods). The
319 original models show Jaccard similarity of 0.27 for the set of metabolites, while the reduced
320 models have Jaccard similarity of 0.26. A similar observation was made comparing bacterial
321 models of *E. coli*, *M. tuberculosis*, and *N. pharaonis* for which at least 95% of the metabolite
322 names could be translated to a common name space. Here, we found Jaccard similarity across

323 the set of metabolites of 0.19 for the original models and 0.16 in the reduced models. These
324 finding demonstrated that the reduction keeps the differences between the original models
325 largely unchanged in comparison to the differences between the reduced models across
326 organisms.

327 Predictions of specific growth rate from reduced models

328 To showcase the benefit of the reduction approach, we considered the reduced models that still
329 include the metabolites (i.e. species) participating in the biomass reactions from the original
330 model (with specified irreversibility). This allows us to compare the simulated specific growth
331 rate between the original and reduced models. The resulting reduced models included 4% fewer
332 metabolites in the model of *A. thaliana* to 28% in the model of *M. musculus* (Fig. 4b). Our
333 findings demonstrate that optimal specific growth rate predicted by the original models are
334 exact match for those of the reduced models (Fig. 4a). Thus, this analysis showcases that the
335 proposed property can be used to remove some well-defined balanced complexes (e.g. those
336 that do not include the building blocks of biomass) without affecting specific growth rates,
337 thus, allowing more targeted applications.



338

339 **Figure 4. Prediction of specific growth rate in original and reduced models.** For direct
340 comparison it is ensured that metabolites that comprise the biomass reaction in the original
341 model remain in the reduced model. **(a)** Specific growth rate estimated from the original and
342 reduced models assuming arbitrary kinetics. The red marked data point are two overlapping
343 points, as shown by the inlay on a smaller scale. **(b)** Model reduction on the level of
344 metabolites.

345 **Analyses of flux variability and essentiality of reactions**

346 Next, we employed the reduced models used in the prediction of specific growth rates to
347 investigate the difference in the ranges derived from flux variability analysis³⁶. To this end,
348 we calculated the ranges of reactions that are present in the reduced and original model
349 following standard procedure^(36 Methods). We found that seven of the reduced models showed
350 the same flux ranges at the optimal specific growth rate determined from FBA as those in the
351 original model. In the remaining five models of *C. reinhardtii*, *M. acetivorans*, *M. tuberculosis*,
352 *T. maritima* and *S. cerevisiae*, 71% to 97% of reactions shared between reduced and original
353 model had the same flux ranges at the optimal specific growth rate determined from FBA as
354 those in the original model (Supplementary Figure 4). For the remaining reactions, we observed
355 that in *C. reinhardtii* 94% showed lower flux ranges, while all remaining reactions for *T.*
356 *maritima* showed larger flux ranges. In models of *M. acetivorans*, *M. tuberculosis* and *T.*
357 *maritima* we found that 47% to 76% of the remaining reactions showed larger flux ranges in
358 the reduced models in comparison to the original. The reason why fluxes of some reactions are
359 larger is because the steady state flux distributions of the original network are also steady state
360 flux distributions in the reduced network; however, the reduced network may admit additional
361 steady states (see Methods). These findings demonstrate that the model reduction leaves the
362 flux variability properties (largely) unchanged.

363 We also inspected the extent to which the reduction affects the predictions of reaction
364 essentiality. To this end, we determined the essential reactions in the reactions shared between
365 the reduced and original models. We found that every reaction that is shared between an
366 original model and its reduced counterpart and is essential in the original model is also essential
367 in the reduced. In addition, the set of reactions introduced during model reduction, e.g. reaction
368 $A \rightarrow C$, introduced by removal of balanced complex B from the path $A \rightarrow B \rightarrow C$,
369 contains no essential reactions for the models of *A. niger* and *N. pharaonis*. In contrast, for the
370 models of *M. acetivorans* and *T. maritima* all reactions in these sets are essential. For the
371 remaining models, the percentage of essential reactions in the set of introduced reactions is
372 between 19% and 50%. The essentiality of reactions introduced during model reduction likely
373 results from lumping of at least one essential reaction in the original model. Therefore, we
374 conclude that the proposed reduction does not alter the findings regarding the essentiality of
375 shared reactions and can be used to infer biological role of reactions.

376 **Conclusion**

377 The constraint-based modelling framework provides a powerful suite of approaches to study
378 the genotype-to-phenotype mapping not only in a single cell, but also across multiple
379 unicellular organisms in a microbial community and interconnected tissues in a multi-cellular
380 organism. However, these advanced applications are associated to increases in the model size
381 which lead to computational and numerical issues in predicting phenotypes of interest. Here,
382 we proposed a fully automated (i.e. unbiased) approach for reduction of models with arbitrary
383 or mass action kinetics at steady state. The approach is based on identifying balanced
384 complexes which contain either a single outgoing reaction, in the case of arbitrary kinetics, or
385 more than one outgoing reaction, for mass action kinetics. We also show that the structural
386 condition can be efficiently identified in large-scale networks, assuming they operate at steady
387 state. Moreover, such balanced complexes can be safely removed from the network as their

388 removal translates into identification of substitution of variables which preserves the steady-
389 state flux distributions of the original model. In addition, the variable substitution can be
390 graphically represented by rewriting the network, leading to a reduced network, and can be
391 carried out without knowledge of kinetic parameters (in the case of mass action kinetics). Most
392 importantly, if a species appears only in balanced complexes, it can be removed from the
393 network and, under the assumption of mass action kinetic, its steady-state concentration can be
394 represented as functions of the steady-state concentrations of the metabolites that remain in the
395 reduced network.

396 Our extensive analysis of genome-scale kinetic models endowed with mass action show that
397 more than 99% of the metabolites can be removed following the proposed reduction. In
398 addition, since the approach is constraint-based, it also allows us to examine if reaction
399 reversibility or assumption on cellular tasks (e.g. growth) that are optimized have an effect on
400 the size of the reduced model, in terms of number of species. The analysis of genome-scale
401 metabolic models across kingdoms of life show that reaction reversibility and assumption of
402 kinetics have the largest effect on the size of the reduced models, leading to up to 85% reduction
403 in the number of species. Nevertheless, we show that if the reduction is performed such that no
404 metabolite participating in the biomass reaction is removed, the reduced model is not affected
405 with respect to predicted growth phenotypes.

406 We would like to emphasize that once the balanced complexes are identified, it is a choice of
407 the modeller which balanced complexes should be removed in the specific analysis case. For
408 instance, we showed that the removal of the balanced complexes, that do not include species
409 that participate in a biomass reactions, does not affect the prediction of specific growth rates.
410 In this scenario, we also showed that the results from flux variability analysis and predictions
411 of essential reactions in reduced and original models are in very good agreement.

412 Since the proposed approach is based on a property that can be efficiently determined even in
413 large-scale networks, it provides the means for reduction of multi-tissue and microbial
414 community models. Moreover, it opens the possibility to study the relationship of key
415 properties, such as robustness and multistationarity, between the original and reduced models.
416 However, these applications will have to ensure imposing additional constraints on the removal
417 of the balanced complexes that do not affect the conservation laws in the network. Finally, our
418 approach opens the possibility for unbiased model reduction by seeking to identify other types
419 of structural motifs in large-scale metabolic networks.

420 **Methods**

421 **Models and their processing**

422 The genome-scale metabolic models of twelve organisms (Supplementary Table S1), were
423 obtained from their original publications^{37–48}. The blocked reactions, reactions with absolute
424 flux values less than $10^{-9} \text{ mmol/gDW/h}$, in the metabolic network were determined by Flux
425 Variability Analysis⁴⁹ and were removed from the original models. Each reversible reaction
426 was split into two irreversible reactions. Two cases for the irreversible reactions originally
427 declared in the model were considered: (1) all were treated as reversible (and were split, as
428 aforementioned) or (2) were maintained as irreversible. The lower bounds for the irreversible
429 reactions were set to zero, while the upper bounds were fixed to the maximum of the upper
430 bounds in the original model. Optimum biomass was determined per Flux Balance Analysis⁵⁰
431 with the assumed reaction reversibility.

432 **Identification of balanced complexes**

433 Let Y denote the non-negative matrix of complexes, with rows denoting species and columns
434 representing complexes. The entry y_{ij} denotes the stoichiometry with which species i enters
435 the complex j . Let A denote the incidence matrix of the directed graph with nodes representing

436 complexes and edges denoting reactions. The rows of A denote the complexes and its column
437 stand for the reactions. Since the graph is directed, each column of A has precisely one -1 and
438 one 1 entry, corresponding to the substrate and product complexes of the respective reaction.
439 The stoichiometric matrix is then given by $N = YA$.

440 The sum of fluxes around the complex i is given by the i th entry of the vector Av , denoted by
441 $[Av]_i$. A complex is balanced in the set of flux distributions $S =$
442 $\{v | Nv = 0, v_{min} \leq v \leq v_{max}\}$ if for every $v \in S$, it holds that $[Av]_i = 0$. This condition can
443 be verified by determining that the minimum and maximum values of $[Av]_i$ equal to 0 for each
444 complex i , separately. The latter can be ensured by solving two linear programs:

$$445 \quad \min / \max [Av]_i$$

446 s.t.

$$447 \quad YAv = Nv = 0$$

$$448 \quad v_{min} \leq v \leq v_{max}.$$

449 The dependence of balanced complexes on the flux bounds is addressed in follow-up studies
450 ⁵¹.

451 **Removal of balanced complexes**

452 Suppose that the complex y is balanced and that it participates in l incoming and m outgoing
453 reactions as a product and substrate complex, respectively. Let y_{i_1}, \dots, y_{i_l} and y_{j_1}, \dots, y_{j_m} denote
454 the substrate and product complexes of the l incoming and m outgoing reactions.

455 Let us assume that $m = 1$, i.e., the complex y is incident on only one outgoing reaction. Due
456 to the balancing of y , $v_{j_1} = \sum_{p=1}^l v_{i_p}$. The removal of the complex y without affecting the
457 steady-state fluxes entails: (i) removal of the $l + 1$ reactions incident on y from the original

458 network and (ii) insertion of l reactions with a substrate complex from y_{i_1}, \dots, y_{i_l} and a product
 459 complex y_{j_1} . This amounts to substituting every occurrence of v_{j_1} by $\sum_{p=1}^l v_{i_p}$, preserving
 460 steady-state flux solutions (i.e. the reduced network includes all steady-state flux solutions of
 461 the original).

462 Let us now assume that $m \geq 1$ and that the network is endowed with mass action kinetics. The
 463 flux of a reaction i with complex $y_{(i)}$ as a substrate is given by $v_i = k_i x^{y_{(i)}}$, where $x^{y_{(i)}} =$
 464 $\prod_j x_j^{y_{ji}}$ and y_{ji} denotes the stoichiometric coefficient of species j in the complex $y_{(i)}$. Due to
 465 complex balancing, then, $x^{y_{(i)}} \sum_{q=1}^m k_{j_q} = \sum_{p=1}^l k_{i_p} x^{y_{(i_p)}}$. The removal of the complex $y_{(i)}$
 466 without affecting the steady-state values x^{y_i} of the complexes entails: (i) removal of the $l + m$
 467 reactions incident on $y_{(i)}$ from the original network and (ii) insertion of ml reactions with a
 468 substrate complex from $y_{(i_1)}, \dots, y_{(i_l)}$ and a product complex from $y_{(j_1)}, \dots, y_{(j_m)}$. The rate
 469 constant of the reaction with $y_{(i_p)}$ and $y_{(j_q)}$ as substrate and product complexes, respectively,
 470 is given by $\frac{k_{i_p} k_{j_q}}{\sum_{q=1}^m k_{j_q}}$. This amounts to substituting every occurrence of $x^{y_{(i)}}$ by

471 $\sum_{p=1}^l \frac{k_{i_p}}{\sum_{q=1}^m k_{j_q}} x^{y_{(i_p)}}$ in $NK\varphi(x) = 0$, preserving the steady-state flux solutions with respect to
 472 $\varphi(x)$ (rather than fluxes, in the case for arbitrary kinetics, above). Note that $\varphi(x)$ is a vector
 473 collecting x^y over all complexes, while K is the matrix with as many rows as reactions and as
 474 many columns as complexes, whose entry k_{ij} corresponds to the rate constant of the reaction i
 475 having complex j as a substrate or zero, otherwise.

476 **Preservation of steady states in the reduction process**

477 Let i index any species/metabolite and v be any steady state flux distribution. It follows from
 478 the steady state property $Nv = YAv = 0$ that $[YAv]_i = 0$; hence $\sum_j Y_{ij} [Av]_j = 0$, where Y_{ij}
 479 is the stoichiometric coefficient by which metabolite i participates in complex j .

480 Let us consider a single elimination step in this process, in which a particular balanced
481 complex, say k , is being removed as explained above. Due to the specific way this removal
482 was defined, the algebraic sum of fluxes for any complex j in the reduced network, that
483 is, $[Av]_j$ remains intact, while this sum for the removed complex k , that is, $[Av]_k$ equals zero
484 like that of any other balanced complex. It follows that the steady state equation for
485 metabolite i , that is, $\sum_j Y_{ij} [Av]_j = \sum_{j \neq k} Y_{ij} [Av]_j + Y_{ik} [Av]_k = 0$ still holds after the
486 elimination.

487 Since the same argument holds for any arbitrary metabolite i , it follows that the whole
488 metabolic network will remain at steady state after each removal step. Therefore, any steady
489 state of the original network is conserved at every elimination step and hence, all along the way
490 up to the last reduced model.

491 **Correspondence of conservation laws**

492 The removal of a balanced complex corresponds structurally to substituting of any directed
493 path of two reactions, N_i and N_j , on which the balanced complex is the middle node, with
494 another reaction, given by reaction vector $N_i + N_j$. Clearly, $N_i + N_j \in \text{span}(\{N_i, N_j\})$. It
495 follows that every new reaction in the reduced network lies in the column span of N . Denoting
496 the stoichiometry matrix for the reduced network by \underline{N} , $\text{im}(\underline{N}) \subseteq \text{im}(N)$ yields $\ker(N^T) \subseteq$
497 $\ker(\underline{N}^T)$. Therefore, for every conservation law, $\lambda^T x = \theta$ that satisfies $\lambda \in \ker(N^T)$, one also
498 has $\lambda \in \ker(\underline{N}^T)$, which means the conservation law is preserved in the reduced network. .
499 However, a conservation law $\mu^T x = \theta$ in the reduced network may not necessarily correspond
500 to one of the original network, unless further constraints are imposed on the balanced
501 complexes being removed.

502 **Predictions of specific growth rates**

503 We calculate optimal specific growth rates by flux balance analysis (FBA) in models with
504 considered irreversibility and compare the predictions before and after removal of balanced
505 complexes. Blocked reactions are removed from the original network and each reversible
506 reaction is split into two irreversible reactions. To avoid cases where no biomass production is
507 ensured in the original model after removal of blocked reactions due to numerical issues, we
508 set the lower bound of the biomass reaction to 5% of the optimal biomass obtained from the
509 model including blocked reactions. In addition, we ensure that the biomass reaction, whose
510 flux is optimized during FBA, is still included in the reduced model. Therefore, we only remove
511 balanced complexes that do not include metabolites (i.e. species) participating in the biomass
512 reactions from the original model.

513 **Analysis of flux variability and essentiality of reactions**

514 We conducted flux variability analysis³⁶ at 99% of optimal biomass for all reactions that appear
515 in both the original and reduced models considering any kinetic. We then classified the
516 reactions into those that do and do not show differences in the flux ranges between each original
517 and corresponding reduced model. Similar analysis was conducted with respect to reaction
518 essentiality: A reaction that appears in both an original and corresponding reduced model was
519 knocked out and the effect on growth was examined. The reactions were classified as those that
520 are essential or not in each model.

521 **Data access**

522 The approach is implemented and available together with all data needed to reproduce the
523 findings at https://github.com/ankueken/network_reduction_by_balanced_complexes.

524

525 **Acknowledgments**

526 Z.N and D.L are supported by the Max Planck Society.

527

528 **Author contributions**

529 Conceptualization: Z.N., data collection: A.K., formal analysis: A.K., investigation: A.K.,
530 Z.N., software: A.K., P.W., validation: A.K., writing – original draft: Z.N., writing – reviewing
531 and editing: A.K., P.W., D.L., Z.N.

532

533 **Competing interests**

534 Authors declare no competing interests.

535

536 **References**

- 537 1. Fang, X., Lloyd, C. J. & Palsson, B. O. Reconstructing organisms in silico: genome-
538 scale models and their emerging applications. *Nature Reviews Microbiology* (2020).
539 doi:10.1038/s41579-020-00440-4
- 540 2. Silverbush, D. & Sharan, R. A systematic approach to orient the human protein–
541 protein interaction network. *Nat. Commun.* (2019). doi:10.1038/s41467-019-10887-6
- 542 3. Thompson, D., Regev, A. & Roy, S. Comparative Analysis of Gene Regulatory
543 Networks: From Network Reconstruction to Evolution. *Annu. Rev. Cell Dev. Biol.*
544 (2015). doi:10.1146/annurev-cellbio-100913-012908
- 545 4. Bordbar, A., Monk, J. M., King, Z. A. & Palsson, B. O. Constraint-based models
546 predict metabolic and associated cellular functions. *Nat. Rev. Genet.* **15**, 107–120
547 (2014).
- 548 5. Stanford, N. J. *et al.* Systematic construction of kinetic models from genome-scale
549 metabolic networks. *PLoS One* (2013). doi:10.1371/journal.pone.0079195

- 550 6. Chindelevitch, L., Trigg, J., Regev, A. & Berger, B. An exact arithmetic toolbox for a
551 consistent and reproducible structural analysis of metabolic network models. *Nat.*
552 *Commun.* (2014). doi:10.1038/ncomms5893
- 553 7. Khodayari, A. & Maranas, C. D. A genome-scale Escherichia coli kinetic metabolic
554 model k-ecoli457 satisfying flux data for multiple mutant strains. *Nat Commun* **7**,
555 13806 (2016).
- 556 8. Radulescu, O., Gorban, A. N., Zinovyev, A. & Noel, V. Reduction of dynamical
557 biochemical reactions networks in computational biology. *Frontiers in Genetics*
558 (2012). doi:10.3389/fgene.2012.00131
- 559 9. Singh, D. & Lercher, M. J. Network reduction methods for genome-scale metabolic
560 models. *Cellular and Molecular Life Sciences* (2020). doi:10.1007/s00018-019-03383-
561 z
- 562 10. Tefagh, M. & Boyd, S. P. Metabolic network reductions. *bioRxiv* 499251 (2019).
563 doi:10.1101/499251
- 564 11. Sambamoorthy, G. & Raman, K. MinReact: a systematic approach for identifying
565 minimal metabolic networks. *Bioinformatics* (2020).
566 doi:10.1093/bioinformatics/btaa497
- 567 12. Jonnalagadda, S. & Srinivasan, R. An efficient graph theory based method to identify
568 every minimal reaction set in a metabolic network. *BMC Syst. Biol.* (2014).
569 doi:10.1186/1752-0509-8-28
- 570 13. Clarke, B. L. General method for simplifying chemical networks while preserving
571 overall stoichiometry in reduced mechanisms. *J. Chem. Phys.* (1992).
572 doi:10.1063/1.463911

- 573 14. Sáez, M., Wiuf, C. & Feliu, E. Graphical reduction of reaction networks by linear
574 elimination of species. *J. Math. Biol.* (2017). doi:10.1007/s00285-016-1028-y
- 575 15. Feliu, E. & Wiuf, C. Variable elimination in chemical reaction networks with mass-
576 action kinetics. *SIAM J. Appl. Math.* (2012). doi:10.1137/110847305
- 577 16. Feliu, E., Lax, C., Walcher, S. & Wiuf, C. Quasi-steady state and singular perturbation
578 reduction for reaction networks with non-interacting species. (2019).
- 579 17. Radulescu, O., Gorban, A. N., Zinovyev, A. & Lilienbaum, A. Robust simplifications
580 of multiscale biochemical networks. *BMC Syst. Biol.* (2008). doi:10.1186/1752-0509-
581 2-86
- 582 18. Rao, S., der Schaft, A. van, Eunen, K. van, Bakker, B. M. & Jayawardhana, B. A
583 model reduction method for biochemical reaction networks. *BMC Syst. Biol.* (2014).
584 doi:10.1186/1752-0509-8-52
- 585 19. Roussel, M. R. & Fraser, S. J. Invariant manifold methods for metabolic model
586 reduction. *Chaos* (2001). doi:10.1063/1.1349891
- 587 20. Sunnåker, M., Cedersund, G. & Jirstrand, M. A method for zooming of nonlinear
588 models of biochemical systems. *BMC Syst. Biol.* (2011). doi:10.1186/1752-0509-5-140
- 589 21. Danø, S., Madsen, M. F., Schmidt, H. & Cedersund, G. Reduction of a biochemical
590 model with preservation of its basic dynamic properties. *FEBS J.* (2006).
591 doi:10.1111/j.1742-4658.2006.05485.x
- 592 22. Schmidt, H., Madsen, M. F., Danø, S. & Cedersund, G. Complexity reduction of
593 biochemical rate expressions. *Bioinformatics* (2008).
594 doi:10.1093/bioinformatics/btn035
- 595 23. Feliu, E. & Wiuf, C. Simplifying biochemical models with intermediate species. *J. R.*

- 596 *Soc. Interface* (2013). doi:10.1098/rsif.2013.0484
- 597 24. Röhl, A. & Bockmayr, A. A mixed-integer linear programming approach to the
598 reduction of genome-scale metabolic networks. *BMC Bioinformatics* (2017).
599 doi:10.1186/s12859-016-1412-z
- 600 25. Erdrich, P., Steuer, R. & Klamt, S. An algorithm for the reduction of genome-scale
601 metabolic network models to meaningful core models. *BMC Syst. Biol.* (2015).
602 doi:10.1186/s12918-015-0191-x
- 603 26. Ataman, M., Hernandez Gardiol, D. F., Fengos, G. & Hatzimanikatis, V. redGEM:
604 Systematic reduction and analysis of genome-scale metabolic reconstructions for
605 development of consistent core metabolic models. *PLoS Comput. Biol.* (2017).
606 doi:10.1371/journal.pcbi.1005444
- 607 27. Baroukh, C., Muñoz-Tamayo, R., Steyer, J. P. & Bernard, O. DRUM: A new
608 framework for metabolic modeling under non-balanced growth. Application to the
609 carbon metabolism of unicellular microalgae. *PLoS One* (2014).
610 doi:10.1371/journal.pone.0104499
- 611 28. Burgard, A. P., Nikolaev, E. V., Schilling, C. H. & Maranas, C. D. Flux coupling
612 analysis of genome-scale metabolic network reconstructions. *Genome Res.* (2004).
613 doi:10.1101/gr.1926504
- 614 29. Pantea, C., Gupta, A., Rawlings, J. B. & Craciun, G. The QSSA in chemical kinetics:
615 As taught and as practiced. in *Natural Computing Series* (2014). doi:10.1007/978-3-
616 642-40193-0_20
- 617 30. Davidi, D. *et al.* Global characterization of in vivo enzyme catalytic rates and their
618 correspondence to in vitro kcat measurements. *Proc Natl Acad Sci U S A* **113**, 3401–

- 619 3406 (2016).
- 620 31. Müller, S. & Regensburger, G. Generalized mass action systems: Complex balancing
621 equilibria and sign vectors of the stoichiometric and kinetic-order subspaces. *SIAM J.*
622 *Appl. Math.* (2012). doi:10.1137/110847056
- 623 32. Neigenfind, J., Grimbs, S. & Nikoloski, Z. On the relation between reactions and
624 complexes of (bio)chemical reaction networks. *J. Theor. Biol.* (2013).
625 doi:10.1016/j.jtbi.2012.10.016
- 626 33. Shinar, G. & Feinberg, M. Structural sources of robustness in biochemical reaction
627 networks. *Science (80-.)*. **327**, 1389–1391 (2010).
- 628 34. Feinberg, M. Chemical reaction network structure and the stability of complex
629 isothermal reactors - I. The deficiency zero and deficiency one theorems. *Chem. Eng.*
630 *Sci.* **42**, 2229–2268 (1987).
- 631 35. Khodayari, A., Zomorodi, A. R., Liao, J. C. & Maranas, C. D. A kinetic model of
632 *Escherichia coli* core metabolism satisfying multiple sets of mutant flux data. *Metab.*
633 *Eng.* **25**, 50–62 (2014).
- 634 36. Gudmundsson, S. & Thiele, I. Computationally efficient flux variability analysis. *BMC*
635 *Bioinformatics* (2010). doi:10.1186/1471-2105-11-489
- 636 37. Andersen, M. R., Nielsen, M. L. & Nielsen, J. Metabolic model integration of the
637 bibliome, genome, metabolome and reactome of *Aspergillus niger*. *Mol. Syst. Biol.*
638 (2008). doi:10.1038/msb.2008.12
- 639 38. Arnold, A. & Nikoloski, Z. Bottom-up Metabolic Reconstruction of Arabidopsis and
640 Its Application to Determining the Metabolic Costs of Enzyme Production. *Plant*
641 *Physiol.* **165**, 1380–1391 (2014).

- 642 39. Zhang, Y. *et al.* Three-dimensional structural view of the central metabolic network of
643 thermotoga maritima. *Science* (80-.). (2009). doi:10.1126/science.1174671
- 644 40. Lu, H. *et al.* A consensus *S. cerevisiae* metabolic model Yeast8 and its ecosystem for
645 comprehensively probing cellular metabolism. *Nat. Commun.* (2019).
646 doi:10.1038/s41467-019-11581-3
- 647 41. Imam, S. *et al.* A refined genome-scale reconstruction of *Chlamydomonas* metabolism
648 provides a platform for systems-level analyses. *Plant J.* (2015). doi:10.1111/tpj.13059
- 649 42. Orth, J. D. *et al.* A comprehensive genome-scale reconstruction of *Escherichia coli*
650 metabolism-2011. *Mol. Syst. Biol.* (2011). doi:10.1038/msb.2011.65
- 651 43. Benedict, M. N., Gonnerman, M. C., Metcalf, W. W. & Price, N. D. Genome-scale
652 metabolic reconstruction and hypothesis testing in the methanogenic archaeon
653 *Methanosarcina acetivorans* C2A. *J. Bacteriol.* (2012). doi:10.1128/JB.06040-11
- 654 44. Feist, A. M., Scholten, J. C. M., Palsson, B., Brockman, F. J. & Ideker, T. Modeling
655 methanogenesis with a genome-scale metabolic reconstruction of *Methanosarcina*
656 *barkeri*. *Mol. Syst. Biol.* (2006). doi:10.1038/msb4100046
- 657 45. Quek, L. E. & Nielsen, L. K. On the reconstruction of the *Mus musculus* genome-scale
658 metabolic network model. *Genome Inform.* (2008). doi:10.1142/9781848163324_0008
- 659 46. Fang, X., Wallqvist, A. & Reifman, J. Development and analysis of an in vivo-
660 compatible metabolic network of *Mycobacterium tuberculosis*. *BMC Syst. Biol.*
661 (2010). doi:10.1186/1752-0509-4-160
- 662 47. Gonzalez, O. *et al.* Characterization of growth and metabolism of the haloalkaliphile
663 *Natronomonas pharaonis*. *PLoS Comput. Biol.* (2010).
664 doi:10.1371/journal.pcbi.1000799

- 665 48. Nogales, J., Palsson, B. & Thiele, I. A genome-scale metabolic reconstruction of
666 *Pseudomonas putida* KT2440: iJN746 as a cell factory. *BMC Syst. Biol.* (2008).
667 doi:10.1186/1752-0509-2-79
- 668 49. Gudmundsson, S. & Thiele, I. Computationally efficient flux variability analysis. *BMC*
669 *Bioinformatics* (2010). doi:10.1186/1471-2105-11-489
- 670 50. Orth, J. D., Thiele, I. & Palsson, B. Ø. O. What is flux balance analysis? *Nat*
671 *Biotechnol* **28**, 245–248 (2010).
- 672 51. Langary, D., Küken, A. & Nikoloski, Z. The unraveling of balanced complexes in
673 metabolic networks. *bioRxiv* 2021.03.23.436554 (2021).
674 doi:10.1101/2021.03.23.436554
- 675